Direct Processing of $PbZr_{0.53}Ti_{0.47}O_3$ Films on Glass and Polymeric Substrates

Yulian Yao[a], Aaron B. Naden[b,c], Fengyuan Zhang[d], David Edwards[d], Pooran Joshi[e], Brian J. Rodriguez[d], Amit Kumar[c], Nazanin Bassiri-Gharb[a,f]

[a]*School of Materials Science and Engineering, Georgia Institute of Technology, Atlanta, Georgia, United States*
[b]*School of Chemistry, University of St Andrews, St Andrews, United Kingdom*
[c]*Centre for Nanostructured Media, School of Mathematics and Physics, Queen's University Belfast, Belfast, United Kingdom*
[d]*School of Physics and Conway Institute of Biomolecular and Biomedical Research, University College Dublin, Belfield, Dublin 4, Ireland*
[e]*Materials Science and Technology Division, Oak Ridge National Laboratory, Oak Ridge, Tennessee, United States*
[f]*G.W. Woodruff School of Mechanical Engineering, Georgia Institute of Technology, Atlanta, Georgia, United States*

Abstract

This work reports on direct crystallization of $PbZr_{0.53}Ti_{0.47}O_3$ (PZT) thin films on glass and polymeric substrates, through the use of pulsed thermal processing (PTP). Specifically a xenon flash lamp is used to deliver pulses of high intensity, short duration broadband light to the surface of a chemical solution deposited thin film, resulting ultimately in the crystallization of the film. Structural analysis by X-ray diffraction and transmission electron microscopy show the existence of perovskite structure in nano-sized grains ($\leq 5nm$). Local functional analysis by band excitation piezoelectric spectroscopy and electrostatic force microscopy confirm presence of a ferroelectric phase and retention of voltage-written polarization for multiple days.

Keywords: `direct low-temperature processing, PZT thin films, perovskite, glass substrates, polymeric substrates`

1. Introduction

Perovskite ferroelectric thin films, such as lead zirconate titanate ($PbZr_xTi_{1-x}O_3$, PZT), are extensively studied for their applications in non-volatile memories and

micro-electromechanical-systems (MEMS), including actuators,transducers, and sensors.[1] However, when it comes to incorporating ferroelectric thin films into complementary metal–oxide–semiconductor (CMOS) processes, temperature incompatibility is a major challenge. High-quality ferroelectric thin films require crystallization temperatures above 600°C[2], but CMOS processes cannot withstand temperature above 400°C, mainly due to the use of metallic circuit materials, as well as modification of the dopant profiles within the various layers, resulting in loss of functionalities.[3] Moreover, demand for transparent touching panels and peel-and-stick sensors[4, 5, 6, 7] has greatly increased in recent years. These applications are usually made from flexible polymer and transparent glass substrates, with limited temperature tolerance, comparable often to CMOS devices.

Various efforts have been made to fabricate ferroelectric thin films on glass or polymeric substrates. Indirect methods, such as laser lift-off[8] and printed ribbons[9], involve transferring ferroelectric films, grown on Si or MgO substrates to the substrates needed for the ultimate application. Such delicate methods, however, significantly complicate the fabrication and integration processes due to the additional transfer step. An alternative complex oxide layer transfer technique releases the ferroelectric single crystal layer by etching the sacrificial layer beneath and uses a transfer stamp to transfer single crystal ferroelectric material layer onto targeted substrates[10, 11]. However, the selection of sacrificial material is challenging due to a required low lattice mismatch with the ferroelectric material, and inertness of the ferroelectric material to the etchant used for the sacrificial material. Alternatively, direct processing methods are expected to keep the substrates at relatively low temperatures, while crystallizing ferroelectric materials. An example for crystallization of ferroelectric materials at nano- to micro-scale is provided through heated atomic force microscope (AFM) tip annealing.[12] In this method, a heated AFE tip in contact with a precursor film deposited by chemical routes is used to crystallize PZT nano- to micro-scale features.[12] Although such a method provides extremely high definition for very small features, it is a slow in-series processing technique. An

example for direct crystallizing at macroscale is pulsed laser deposition[13, 14]. This method utilizes a high-temperature laser to raster across the film surface, but it, too, is a very time-consuming serial process. Additionally, PZT films prepared by this method only show good ferroelectric properties when the substrate was kept at 400°C during the laser processing, which can lead to degradation of substrates or other non-thermally robust components of the device.[15]

Here, we report a new technique for direct processing of PZT thin films on glass or polymeric substrates, based on pulsed thermal processing (PTP). PTP or photonic curing, is a processing method using a xenon lamp as the heating source; the Xe plasma delivers a high intensity, short duration (as low as 25 µs) broadband light to generate heating rates as high as $600,000$°C/s.[16] The pulse duration is much shorter than the thermal equilibrium time of the substrates, resulting in a large temperature gradient across the sample thickness, thus enabling the use of temperature sensitive substrates such as glass, polymer, and fabric.[17] Additionally, PTP is compatible with roll-to-roll processing, making it ideal for industrial applications, where large area processing and low cost are further requirements.

2. Experimental Section

PZT with Zr to Ti ratio of 53:47 at the morphotropic phase boundary (MPB) is selected as the representative ferroelectric material, based on its highest electromechanical response among PZT solid solutions.[18]. The PZT precursor solutions were prepared by a 2-methoxyethanol route, described previously.[19] Zirconium (IV) propoxide solution, $Zr(OCH_2CH_2CH_3)_4$ 70 wt.% in 1-propanol (Sigma-Aldrich, Inc.), and titanium (IV) propoxide, $Ti[OCH(CH_3)_2]_4$ 97% (Sigma-Aldrich, Inc.) were dissolved in 2-methoxyethanol (2-MOE), $CH_3OCH_2CH_2OH$ 99.9% (Sigma-Aldrich, Inc.) and stirred at 115 °C for 30 minutes in Argon environment. In a separate flask, lead acetate tri-hydrate, $Pb(CH_3CO_2)_2{\cdot}3H_2O$ 99.99% on a trace metals basis (Sigma-Aldrich, Inc.) was dissolved in 2-MOE and vacuum dried at 120 °C until water was fully distilled. Subsequently, the

mixture of Zr and Ti precursors was added to the Pb flask and the obtained solution was stirred for 4 hours at 115 °C. Finally, the solution was adjusted to 0.4 M by adding 2MOE or vacuum distillation.

The substrates used in this work were platinized soda-lime glass slides and polymeric Kapton substrates. The PZT precursor solution were spun coated onto the substrates at 3000 rpm for 30 s. As-deposited films were pyrolyzed on a hot plate at 400 °C for 1 minute. Crystallization was carried out with PulseForge 3300 processing system from NovaCentrix PulseForge 3300 processing system is designed for processing high melting temperature materials on low-temperature substrates. For PZT thin films on glass slides, pulse voltages ranging from 325 V to 450 V, pulse durations of 500 µs, and pulse counts from 10 to 100 were investigated. For PZT thin films on polymeric substrates, pulse voltages ranging from 200 V to 325 V, pulse durations of 250 µs, and pulse counts from 10 to 100 were investigated.

The piezoelectric and ferroelectric properties of the crystallized films were studied via piezoresponse force microscopy (PFM) and band excitation piezoelectric spectroscopy (BEPS) techniques using an Asylum Research Cypher atomic force microscope (AFM). Conducting tips (PPP-EFM, Nanosensors) tips with a nominal resonance frequency of 75 kHz and 2.8 N/m spring constant were used for the measurements. Single frequency vertical PFM (VPFM) images were obtained using an external lock-in amplifier (HF2LI, Zurich Instruments) through excitation of the tip near the contact resonance frequency (300 kHz) at an AC voltage of 2 V. BEPS measurements were performed using a National Instruments module controlled by a Labview interface. The DC voltage waveform used at each pixel consisted of a 64-step pulsed triangular wave which started and ended at 0 V, with a ±10V and ±25V range for the samples grown on glass and Kapton, respectively. The piezoresponse was excited and measured both during ("write") and between ("read") each pulse, using a band excitation signal with an AC voltage of 1 V amplitude and a 150 kHz bandwidth centered around the contact resonance frequency. Electrostatic force microscopy (EFM) was carried out using the same PPP-EFM tips, excited with an AC voltage of

1 V at 30 kHz. The EFM response was collected using the internal Cypher lock-in amplifier.

3. Results and discussion

3.1. Optimizing the processing parameters

To control the heat transferred to the sample, multiple parameters in the PTP waveform can be adjusted. From the example waveform (Figure 1), the adjustable parameters include pulse voltage (the intensity of applied pulse), pulse count (the number of pulses applied), and pulse duration for both preheating and crystallization steps. A preheat pulse (dotted line) with longer pulse duration and lower voltage is used to raise the temperature of the whole sample. A preheat set of 220 V, 1 ms, and 10 pulses were applied to all samples. After preheating, samples were dwelled for 1 s, and then pulses with shorter duration and higher intensity were applied to create a large temperature gradient from the surface to the substrate. The effects of pulse count, pulse voltage, and pulse duration on the crystallization of PZT thin films are investigated. Pulse voltage determines the energy delivered onto the surface of the sample. Pulse voltages lower than critical values can result in lack of crystallization or incomplete crystallization of the perovskite phase. Higher pulse voltages could cause overheating and damage to substrates. Moreover, a high intensity pulse of short duration can also lead to explosive evaporation of organics, creation of non uniform films and/or extensive defects in PZT films. Similarly, longer pulse duration allows for more heat to be transferred to the sample while lowering the temperature gradient from the surface to the substrate, which could damage the substrates. The energy applied to the sample also increases with increasing number of pulses.[20] Pulse durations of 500 µs were used for crystallizing PZT thin films on glass substrates. Pulse duration of 250 µs were used for PZT thin films on polymeric substrates, since preliminary studies (not reported here) found that longer duration pulses damage polymeric substrates. The effects of the thickness of the precursor PZT films were also studied, showing that for

PZT films on polymeric substrates, a thicker film (15 layer) show much higher crystallinity than a thinner film (3 layer). Hence, all PZT films on polymeric substrates discussed below are 15-layered.

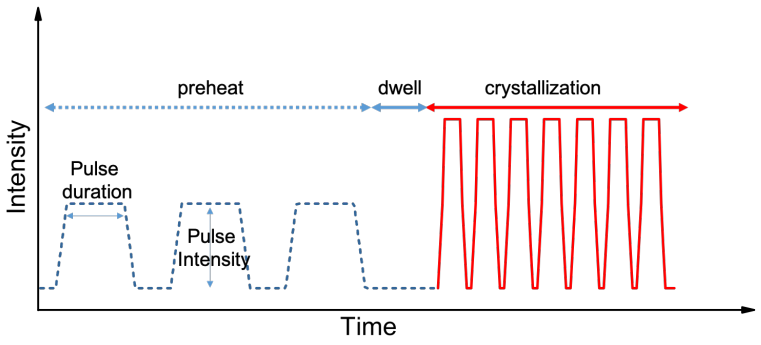

Figure 1: Schematic representation of the applied waveform during pulsed thermal processing, where dotted line stands for the preheat waveform and solid line stands for crystallization waveform. Between preheat step and crystallization step, there is a dwell step to let the heat transfer to substrates so that the substrates can be at a relatively high temperature during crystallization step.

For PZT thin films on glass substrates, pulse voltages of 325 V, 350 V, 400 V, 425 V, and 450 V and pulse counts of 10, 25, 50, and 100 are studied. X-ray diffraction (XRD) patterns (Figure 3) show that a threshold energy is required to crystallize PZT films into perovskite structure. When a relatively low pulse count or voltage is applied, PZT films do not show perovskite phase. With increasing applied energy, PZT films on glass substrates are predominately 111-oriented. However, when the applied energy is further increased, such as the PZT films crystallized with 100 pulses in Figure 2b or 425 V in Figure 2d, 001 and 010 peaks become stronger and the overall orientation changes towards random.

An examination of a cross-sectional area (Figure 4) of a PZT thin film on glass substrate (3L, 400 V, 500 µs, and 10 pulses) with bright field transmission electron microscopy (BF-TEM) revealed nano-crystalline grains. The grain size

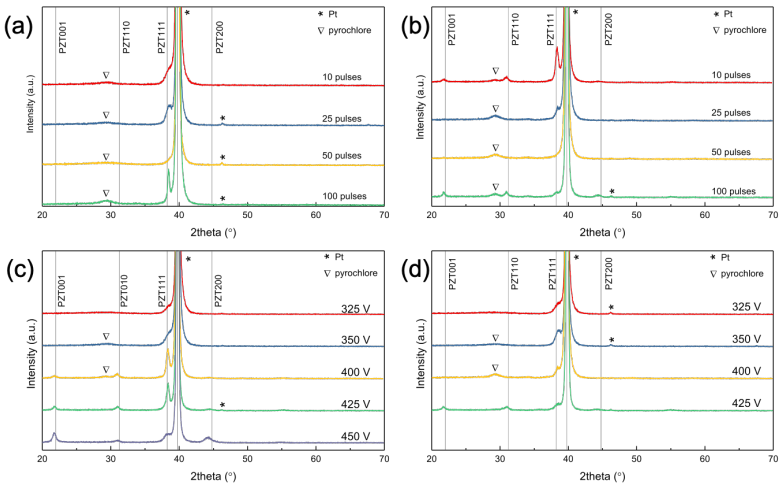

Figure 2: The effects of pulse count and pulse intensity on the developed crystallographic phase in PZT films on glass substrates. X-ray diffraction patterns of PZT thin films processed on glass substrates, and crystallized with (a) 350 V pulse voltage, 500 µs pulse duration, and 10 to 100 pulse counts, (b) 400 V pulse voltage, 500 µs pulse duration, and 10 to 100 pulse counts, (c) 325 to 450 V pulse voltage, 500 µs pulse duration, and 10 pulse counts, and (d) 325 to 425 V pulse voltage, 500 µs pulse duration, and 25 pulse counts.

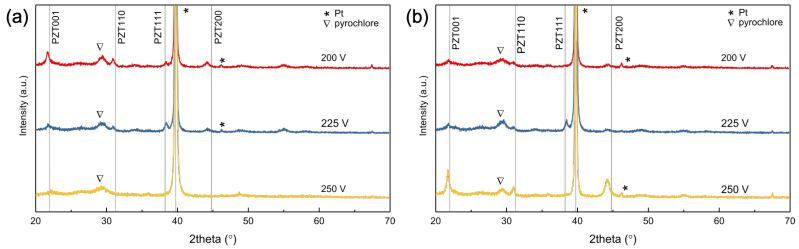

Figure 3: The effects of pulse count and pulse intensity on the developed crystallographic phase in PZT films on Kapton substrates. X-ray diffraction patterns of PZT thin film on Kapton substrates crystallized with 200 V to 250 V pulse voltage, 250 µs pulse duration, and (a) 10 or (b) 25 pulse counts.

140 gradually decreased from bottom of the film, at the interface with the substrate, to the surface of the film. The grain size gradient suggests that the the crystallization is stronger at the PZT-Pt interface, possibly indicating that this is where

This Work	Perovskite[21]	Flourite[22, 13]	Pyrochlore[23]	Other Low Temperature Structures[24]
0.313			d_{311} = 0.316	
0.293/0.292	d_{101} = 0.289	d_{111} = 0.303		0.297
0.268	d_{110} = 0.285	d_{200} = 0.263	d_{400} = 0.262	0.251
	d_{111} = 0.235			

Table 1: *d*-spacings in nanometers for perovskite and other crystallographic phases (fluorite, pyrochlore) in this work and based on literature.

the temperature is higher in the film. The majority of the light emitted from xenon light source has wavelength longer than 800 nm.[25] While no information was found in literature with respect to the PZT film precursor before crystallization, the extinction coefficient of crystallized PZT is lower than 0.001 at wavelengths longer than 800 nm,[26] while the extinction coefficient for Pt films is larger than 5 at this wavelength range.[27] As a result, we consider the PZT films to be almost transparent to the light source, and that most of the energy provided is absorbed by the Pt layer. The high-temperature Pt leads to the initiation of crystallization in the bottom part of the film. When the PZT thin film is crystallized with higher energy (425 V, 500 µs, and 10 pulses), the grain size is more uniform (Figure 4c). From energy-dispersive X-ray spectroscopy (EDX) profile (Figures 4b and d) across the thickness, the composition of the film is also relatively uniform in the direction perpendicular to the substrate. Composition uniformity across the thickness would provide a substantial advantage for PTP over traditional crystallization methods (e.g., furnace or rapid thermal annealing), which can result in chemical fluctuations across the thickness[28, 29] or surface Pb deficiency.[30] Lattice parameters (Table 1) of 0.292 nm and 0.268 nm are extracted from the inset fast Fourier transform (FFT) image (Figure 4a) and are matched to 101 and 110 perovskite PZT planes.[21] *d*-spacings of 0.268 and 0.313 nm are also extracted from the FFT images and correlate well with the corresponding pyrochlore values (less than 3% variation) compared to a number of literature reports (Table 1)) ,[23, 21, 31, 23, 13, 22, 24]

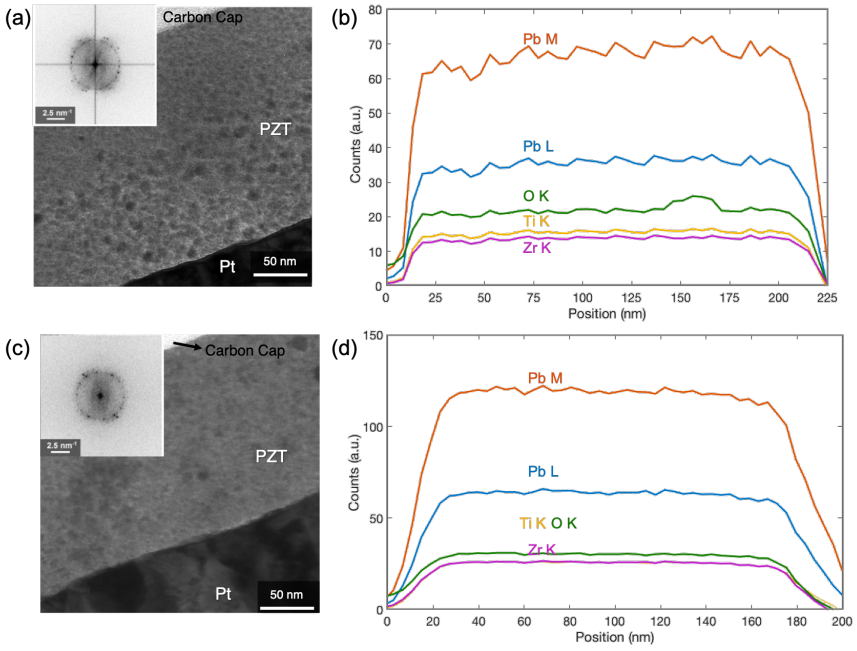

Figure 4: Bright field transmission electron microscopy and corresponding fast Fourier transformation (FFT) images (inserts) of PZT thin films on glass substrates crystallized with (a) 10 pulses at 400 V, each for 500 µs, and (c) 10 pulses at 425 V, each for 500 µs. Energy-dispersive X-ray spectroscopy (EDS) across the thickness of PZT thin films on glass substrate crystallized with (b) 400 V, 500 us, and 10 pulses and (d) 425 V, 500 µs and 10 pulses.

PZT films on polymeric substrates were processed with pulse voltages of 200 V, 225 V, and 250 V and pulse counts of 10 and 25, in order to further limit the provided energy, based on the substrate susceptibility to temperature increase. XRD patterns (Figure 3) show that the PZT films on polymeric substrates have perovskite phase with random orientations, at almost all processing conditions. Compared to the films processed on glass substrates, films on polymeric substrates contain also a higher amount of pyrochlore. This is possibly a result of lower crystallization temperature due to the lower pulse voltage and pulse duration, in order to maintain the substrate integrity. Additionally, due to the substrate's flexibility, the polymer-based samples tend to curl under the applied thermal gradients and undergo non-uniform exposure. As a result, some regions

are closer to the energy source and better-crystallized than others, which might show larger secondary phase content.

3.2. Ferroelectric properties

As discussed above, when lower energy levels are supplied to the samples, the crystallization is initiated at the PZT-Pt interface while the surface at lower crystalline quality than the rest of the film. Since piezoresponse force microscopy (PFM) can characterize only the regions near the sample surface, PZT samples crystallized with higher voltage and pulse counts (3L, 450 V, 500 µs, and 50 pulses) were selected to ensure sufficient surface crystallinity. Figures 5a and 5b show the initial vertical PFM (VPFM) amplitude and phase, respectively, in a $5\mu m \times 5\mu m$ region of the film. In the central $3\mu m \times 3\mu m$ region of the image (as indicated by the dashed line), -10 V was applied from the PFM tip to the left-hand side of the region, while +10 V was applied to the right-hand side. In the subsequently acquired VPFM images (Figures 5c and d), the region written with -10 V displays a reversed phase with respect to the +10 V-written region (and the majority of the surrounding area), implying that the polarization orientation has switched from pointing downward (into the substrate), to upwards (towards the surface of the film). However, some regions appear to have not switched; such regions mostly coincide with the grain boundaries evident in the topography. Aside from the points in close proximity to the grain boundaries, the switched points written with -10 V and +10 V were found to be stable over time within both regions. After over 24 hours, the switched points (Figures 5e and f) show consistent contrast, indicating good retention of ferroelectricity.[32] However, some non-ferroelectric contributions, such as charge injection, can also result in long-lived "switched" states with relaxation time up to days.[33, 34] To rule out the contributions from charge injection, electrostatic force microscopy (EFM) was performed on the electrically-written region (Figures 5g and h). EFM is a dynamic non-contact method that measures the attractive/repulsive force between the surface charge and a tip excited by an AC voltage.[35] No ob-

vious change in the EFM contrast was observed in the written area and hence we conclude that residual surface charge injection does not contribute to the contrast observed in the VPFM amplitude and phase images after writing.

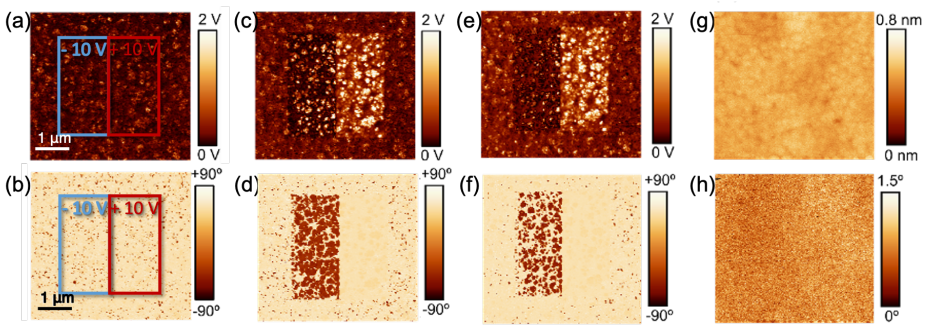

Figure 5: Demonstration of ferroelectric switching on a PZT sample on glass (3L, 450V, 500 µs, and 50 pulses). Initial VPFM (a) amplitude and (b) phase before voltage application, (c) amplitude and (d) phase immediately after applying -10 V from the tip to the left side of the central $3\mu m \times 3\mu m$ region and +10 V to the right side, and (e) amplitude and (f) phase 24 hours after applying voltage. Corresponding EFM (g) amplitude and (h) phase $<$ 1 hour after applying the $\pm$10 V.

Band excitation piezoelectric spectroscopy (BEPS)[36] measurements were also conducted over a similar region of the film. The measurements, reported in Figure 6, show an average response acquired from more than 20 locations on the film surface where similar behaviour occurred. In sweeping from positive to negative applied voltages and back, a hysteretic reversal in VPFM phase (Figure 6b) is observed around $\pm$4 V, which correlates with minima in VPFM amplitude (Figure 5a). The corresponding averaged resonant frequency evolution with applied bias is also shown in Figure 6c, and demonstrates an initial overall decrease between 0 V and +6 V at the beginning of the loop, with a number of spikes and dips around the positive coercive bias, before increasing overall for the remainder of the loop, with spikes appearing again around negative coercive bias. Such spikes around switching typically occur due to the onset of domain nucleation under the cantilever.[37] The underlying increase and decrease in resonance frequency could meanwhile be attributed to material

hardening and softening respectively during hysteresis acquisition.[38] or the effect of bias-induced changes in the absorbate layer.[37] These observations, along with the saturated hysteretic loops and the presence of stable switched domains all confirm the ferroelectric nature of the locations probed on the film.

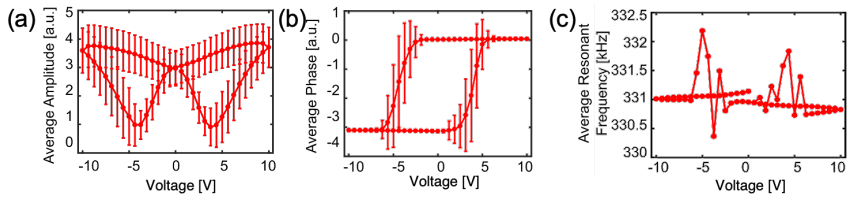

Figure 6: Average of more than 20 read loops for the measured (a) amplitude, (b) phase, and (c) tip-surface contact resonance frequency on a PZT film grown on glass (3L, 450V, 500 µs, and 50 pulses). The loops were measured in band-excitation mode with 1 V amplitude and 150 kHz bandwidth over a 30×30 grid across a $3\mu m \times 3\mu m$ area.

A similar PFM/EFM study to the PZT films on glass was carried out for a film grown on the polymeric substrate (15L, 250 V, 250 µs, and 25 pulses). The corresponding VPFM phase are shown in Figures 7a and 7b. It should be noted that the VPFM amplitude appears lower than for the sample grown on glass, likely due to the variation in measured response between different PFM tips. Here, the left side of the central ($3\mu m \times 3\mu m$) region of the image shown, and +25 V was applied to the right side. The larger bias values where chosen based on preliminary experiments: the films grown on polymer substrates required a higher bias to induce switching. This is because, compared to the glass-grown samples, the polymer-grown samples were thicker and contained a larger amount of pyrochlore. It should also be noted that the larger applied voltages likely contribute to the write-and-read results in other ways, such as charge injection. Observing the subsequent PFM images, the negative applied bias resulted in a reversed VPFM phase (Figure 7d), implying a polarization reversal from downwards to upwards. Compared to the films on the glass substrate, the phase reversal in films on polymeric substrate appears to be much more uniform,

with switching occurring across the full written region. The switched domains are surrounded by a minimum in VPFM amplitude, consistent with the presence of a 180° domain wall, and are stable over more than 24 hours (Figures 7e and f). For both PZT films (grown on glass or polymeric substrates) positive bias appears to result in an enhancement of the VPFM amplitude, compared to VPFM amplitude in the negative voltage-written area. The increase and decrease in amplitude could be due to bias-induced surface changes or ionic motion. Instrumental effects such as the laser spot position or effects of the electronics of the experimental setup, could also result in apparent asymmetry in the polarity-dependence of the PFM response. However, EFM characterization revealed variations in contrast shortly after domain writing (<1 hour) as shown in figures 7g and h, implying possible charge injection or electrostatic related phenomena due to the high voltage applied.[35, 39]

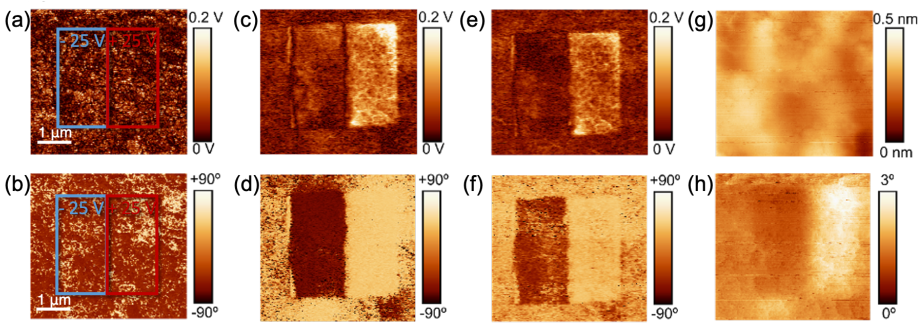

Figure 7: Demonstration of ferroelectric switching on a PZT sample grown via PTP on a flexible polymeric substrate crystallized with 250 V, 250 µs, and 25 pulses. Initial VPFM (a) amplitude and (b) phase before voltage application, (c) amplitude and (d) phase immediately after applying -25 V to the left side of the central $3\mu m \times 3\mu m$ region, and +25 V to the right side, and (e) amplitude and (f) phase 24 hours after applying voltage. Corresponding EFM (g) amplitude and (h) phase acquired $<$ 1 hour after the writing experiments.

In studying the amplitude and phase loop shapes via BEPS in Figure 8a and 8b, a hysteretic piezoresponse is observed, with phase reversal at approximately +13 V and -17 V, accompanied by local minima in the VPFM am-

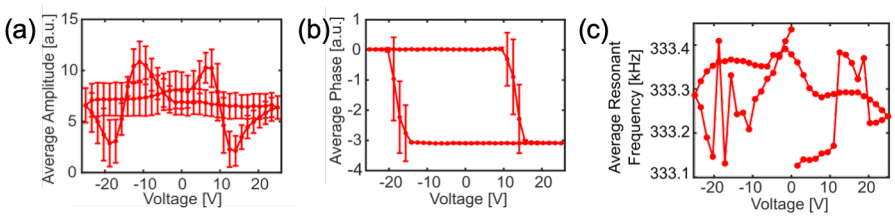

Figure 8: Average of >20 read loops for the measured (a) amplitude, (b) phase, and (c) tip-surface contact resonance frequency on sample grown a polymeric substrate (15L, 250V, 250 µs, and 25 pulses). The loops were measured in band-excitation mode with 1 V amplitude and 150 kHz bandwidth over a 30 × 30 grid across a 3 × 3 µm area, and >20 loops which demonstrated similar switching behaviour in different locations across the grid are selected.

plitude curve. Compared to the results obtained from glass-grown films, the results from polymer-grown films suggest a number of differences in behavior, including an increase in VPFM amplitude before switching. The evolution in resonance frequency meanwhile appears more complex (Figure 8c) compared to the sample grown on glass: an increase at positive bias, before decreasing and then increasing again at negative bias, are accompanied by local hardening at the positive coercive voltage. Based on the large bias voltage applied to the sample, the shape of the amplitude loop and the change in EFM after the writing experiments are consistent with substantial contributions from charge injection. Despite the additional contributions to the apparent local electromechanical response, the stability of the switched domains, the repeatable hysteretic switching behavior and full saturation of phase at both polarities all point towards the ferroelectric nature of the film.

4. Conclusions

In summary, PZT thin films on both glass and polymeric substrates were successfully crystallized by PTP. XRD and TEM show the existence of perovskite PZT, and PFM shows reversible out-of-plane polarization for the PZT films. The PTP crystallized PZT also show good ferroelectric retention for over 24 hrs. By measuring the surface potential and VPFM phase and ampli-

tude after over 24 hrs, the observed electromechanical response and switching is attributed mainly to ferroelectric response, rather than non-ferroelectric contributions from electrostatic, electromechanical, and electrostrictive effects. The successful direct crystallization of PZT thin film demonstrates PTP as an effective technique for crystallization of ferroelectric thin films on transparent and flexible substrates.

References

[1] S. Kim, D. Seol, X. Lu, M. Alexe, Y. Kim, Electrostatic-free piezoresponse force microscopy, Scientific reports 7 (2017) 41657 (2017).

[2] P. T. Tue, Y. Takamura, Lead zirconium titanate films and devices made by a low-temperature solution-based process, Ferroelectrics and Their Applications 3 (2018) 89 (2018).

[3] A. Mehta, M. Gromova, C. Rusu, R. Olivier, K. Baert, C. Van Hoof, A. Witvrouw, Novel high growth rate processes for depositing poly-sige structural layers at cmos compatible temperatures, in: 17th IEEE International Conference on Micro Electro Mechanical Systems. Maastricht MEMS 2004 Technical Digest, IEEE, 2004, pp. 721–724 (2004).

[4] J. A. Rogers, Slice and dice, peel and stick: emerging methods for nanostructure fabrication, ACS nano 1 (3) (2007) 151–153 (2007).

[5] D. Fu, K. Suzuki, K. Kato, H. Suzuki, Dynamics of nanoscale polarization backswitching in tetragonal lead zirconate titanate thin film, Applied physics letters 82 (13) (2003) 2130–2132 (2003).

[6] K. Yamakawa, K. Imai, O. Arisumi, T. Arikado, M. Yoshioka, T. Owada, K. Okumura, Novel $Pb(ZrTi)O_3$ (pzt) crystallization technique using flash lamp for ferroelectric ram (feram) embedded lsis and one transistor type feram devices, Japanese journal of applied physics 41 (4S) (2002) 2630 (2002).

[7] K. Noritake, T. Matsukawa, M. Koh, K.-i. Hara, M. Goto, I. Ohdomari, Site dependence of soft errors induced by single-ion hitting in 64 kbit static random access memory (sram), Japanese journal of applied physics 31 (6B) (1992) L771 (1992).

[8] Y. H. Do, W. S. Jung, M. G. Kang, C. Y. Kang, S. J. Yoon, Preparation on transparent flexible piezoelectric energy harvester based on PZT films by laser lift-off process, Sensors and Actuators A: Physical 200 (2013) 51 (2013).

[9] Y. Qi, J. Kim, T. D. Nguyen, B. Lisko, P. K. Purohit, M. C. McAlpine, Enhanced piezoelectricity and stretchability in energy harvesting devices fabricated from buckled pzt ribbons, Nano letters 11 (3) (2011) 1331 (2011).

[10] S. R. Bakaul, C. R. Serrao, M. Lee, C. W. Yeung, A. Sarker, S.-L. Hsu, A. K. Yadav, L. Dedon, L. You, A. I. Khan, et al., Single crystal functional oxides on silicon, Nature communications 7 (2016) 10547 (2016).

[11] H. Elangovan, M. Barzilay, S. Seremi, N. Cohen, Y. Jiang, L. W. Martin, Y. Ivry, Giant superelastic electromechanical response in flexible ferroelectric batio _3 membranes, arXiv preprint arXiv:2002.08166 (2020).

[12] S. Kim, Y. Bastani, H. Lu, W. P. King, S. Marder, K. H. Sandhage, A. Gruverman, E. Riedo, N. Bassiri-Gharb, Direct fabrication of arbitrary-shaped ferroelectric nanostructures on plastic, glass, and silicon substrates, Advanced Materials 23 (33) (2011) 3786–3790 (2011).

[13] A. P. Wilkinson, J. S. Speck, A. K. Cheetham, S. Natarajan, J. M. Thomas, In situ x-ray diffraction study of crystallization kinetics in $PbZr_{1-x}Ti_xO_3$,(PZT, x= 0.0, 0.55, 1.0), Chemistry of materials 6 (6) (1994) 750 (1994).

[14] A. Rajashekhar, H.-R. Zhang, B. Srowthi, I. M. Reaney, S. Trolier-McKinstry, Microstructure evolution of in situ pulsed-laser crystallized

$Pb(Zr_{0.52}Ti)_{0.48}O_3$ thin films, Journal of the American Ceramic Society 99 (1) (2016) 43 (2016).

[15] S. Bharadwaja, T. Dechakupt, S. Trolier-McKinstry, H. Beratan, Excimer laser crystallized (Pb, La)(Zr, Ti)O_3 thin films, Journal of the American Ceramic Society 91 (5) (2008) 1580 (2008).

[16] P. C. Joshi, T. Kuruganti, S. M. Killough, Impact of pulse thermal processing on the properties of inkjet printed metal and flexible sensors, ECS Journal of Solid State Science and Technology 4 (4) (2015) 3091 (2015).

[17] V. Akhavan, K. Schroder, D. Pope, I. Rawson, A. Edd, S. Farnsworth, Reacting thick-film copper conductive inks with photonic curing, in: Proceedings of the 13th International Symposium on Electronics Packaging (ICEP2013). The Japan Institute of Electronics Packaging (JIEP), 2013 (2013).

[18] S. Mabud, The morphotropic phase boundary in pzt solid solutions, Journal of Applied Crystallography 13 (3) (1980) 211 (1980).

[19] S. J. Brewer, S. C. Williams, C. Z. Deng, A. B. Naden, S. M. Neumayer, B. J. Rodriguez, A. Kumar, N. Bassiri-Gharb, Functional and structural effects of layer periodicity in chemical solution-deposited $Pb(Zr_xTi_{1-x})O_3$ thin films, Journal of the American Ceramic Society 100 (12) (2017) 5561 (2017).

[20] M. S. Rager, T. Aytug, G. M. Veith, P. Joshi, Low-thermal-budget photonic processing of highly conductive cu interconnects based on cuo nanoinks: potential for flexible printed electronics, ACS applied materials & interfaces 8 (3) (2016) 2441–2448 (2016).

[21] J. Joseph, T. Vimala, V. Sivasubramanian, V. Murthy, Structural investigations on $Pb(Zr_xTi_{1-x})O_3$ solid solutions using the x-ray rietveld method, Journal of materials science 35 (6) (2000) 1571 (2000).

[22] D. Kaewchinda, T. Chairaungsri, M. Naksata, S. Milne, R. Brydson, Tem characterisation of PZT films prepared by a diol route on platinised silicon substrates, Journal of the European Ceramic Society 20 (9) (2000) 1277 (2000).

[23] C. K. Kwok, S. B. Desu, Pyrochlore to perovskite phase transformation in sol-gel derived lead-zirconate-titanate thin films, Applied Physics Letters 60 (12) (1992) 1430 (1992).

[24] C. D. Lakeman, Z. Xu, D. A. Payne, On the evolution of structure and composition in sol-gel-derived lead zirconate titanate thin layers, Journal of materials research 10 (8) (1995) 2042 (1995).

[25] NovaCentrix, Pulseforge 3300 datasheet.
URL `https://www.novacentrix.com/products/pulseforge/3300`

[26] S. Majumder, Y. Mohapatra, D. Agrawal, Optical and microstructural characterization of sol/gel derived cerium-doped PZT thin films, Journal of materials science 32 (8) (1997) 2141–2150 (1997).

[27] A. D. Rakić, A. B. Djurišić, J. M. Elazar, M. L. Majewski, Optical properties of metallic films for vertical-cavity optoelectronic devices, Applied optics 37 (22) (1998) 5271–5283 (1998).

[28] A. Dutschke, J. Meinhardt, D. Sporn, Analysis of the phase content and Zr: Ti fluctuation phenomena in PZT sol-gel films with a nominal composition near the morphotropic phase boundary, Journal of the European Ceramic Society 24 (6) (2004) 1579–1583 (2004).

[29] A. Nagai, J. Minamidate, G. Asano, C. J. Choi, C.-R. Cho, Y. Park, H. Funakubo, Conformality of Pb(Zr, Ti)O_3 films deposited on trench structures having submicrometer diameter and various aspect ratios, Electrochemical and solid-state letters 9 (1) (2006) C15–C18 (2006).

[30] I. Gueye, G. Le Rhun, O. Renault, E. Defay, N. Barrett, Electrical response of Pt/Ru/$PbZr_{0.52}Ti_{0.48}O_3$/Pt capacitor as function of lead precursor excess, Applied Physics Letters 111 (22) (2017) 222902 (2017).

[31] X.-h. Du, J. Zheng, U. Belegundu, K. Uchino, Crystal orientation dependence of piezoelectric properties of lead zirconate titanate near the morphotropic phase boundary, Applied physics letters 72 (19) (1998) 2421 (1998).

[32] N. Balke, P. Maksymovych, S. Jesse, A. Herklotz, A. Tselev, C.-B. Eom, I. I. Kravchenko, P. Yu, S. V. Kalinin, Differentiating ferroelectric and nonferroelectric electromechanical effects with scanning probe microscopy, ACS nano 9 (6) (2015) 6484–6492 (2015).

[33] S. Skiadopoulou, S. Kamba, J. Drahokoupil, J. Kroupa, N. Deepak, M. E. Pemble, R. W. Whatmore, Comment on "interesting evidence for template-induced ferroelectric behavior in ultra-thin titanium dioxide films grown on (110) neodymium gallium oxide substrates", Advanced Functional Materials 26 (5) (2016) 642–646 (2016).

[34] N. Deepak, M. A. Caro, L. Keeney, M. E. Pemble, R. W. Whatmore, Interesting evidence for template-induced ferroelectric behavior in ultra-thin titanium dioxide films grown on (110) neodymium gallium oxide substrates, Advanced Functional Materials 24 (19) (2014) 2844–2851 (2014).

[35] J. Son, G. Lee, Y.-H. Shin, Surface charge dynamics on ferroelectric $PbZr_{0.48}Ti_{0.52}O_3$ films responding to the switching bias of electric force microscope, Applied Physics Letters 94 (16) (2009) 162902 (2009).

[36] S. Jesse, S. V. Kalinin, R. Proksch, A. Baddorf, B. Rodriguez, The band excitation method in scanning probe microscopy for rapid mapping of energy dissipation on the nanoscale, Nanotechnology 18 (43) (2007) 435503 (2007).

[37] S. Jesse, P. Maksymovych, S. V. Kalinin, Rapid multidimensional data acquisition in scanning probe microscopy applied to local polarization dynamics and voltage dependent contact mechanics, Applied Physics Letters 93 (11) (2008) 112903 (2008).

[38] A. B. Naden, D. Edwards, S. M. Neumayer, J. G. Guy, B. J. Rodriguez, N. Bassiri-Gharb, A. Kumar, Revealing the interplay of structural phase transitions and ferroelectric switching in mixed phase bifeo3, Advanced Materials Interfaces 5 (21) (2018) 1801019 (2018).

[39] S. Bühlmann, E. Colla, P. Muralt, Polarization reversal due to charge injection in ferroelectric films, Physical Review B 72 (21) (2005) 214120 (2005).